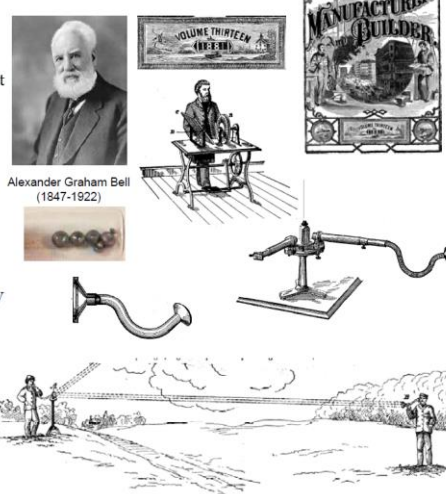


# Optoacoustic (photoacoustic) imaging

## The optoacoustic (photoacoustic) effect

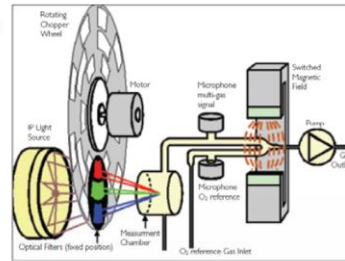
The idea of photoacoustics being used to create acoustic waves by the absorption of light is a relatively old technology. Alexander Graham Bell discovered that you can transmit sound by **flashing** a focused beam of **light** with rotating slotted disk onto **selenium** in 1880. The absorbed energy from the sunlight is transformed into kinetic energy of the sample by energy exchange processes. This results in **local heating** and thus a pressure wave or **sound**. The sound produced from the selenium could then be picked up by a hearing tube. The device received the name **photophone**.



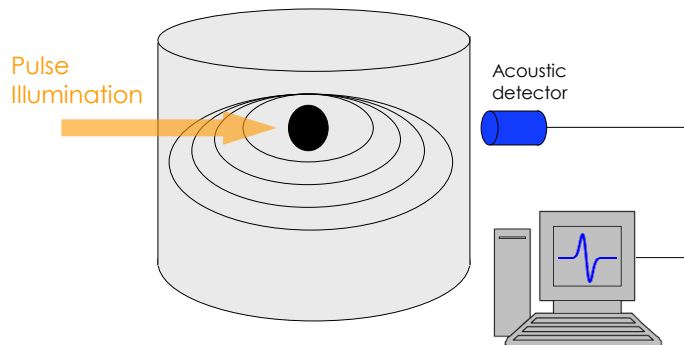
## Main milestones

- 1880 - The photoacoustic (optoacoustic) effect is discovered by A. G. Bell
- 1938 - First practical implementation in gases. CO<sub>2</sub> concentration in N<sub>2</sub> gas was measured by M. L. Vingelov
- 1973 - Practical use of the optoacoustic effect for condensed phase materials was rediscovered simultaneously by A. Rosencwaig (Bell Labs) and A. G. Parker (Johns Hopkins University). A general theory for the optoacoustic effect was developed by Rosencwaig and Gersho and is commonly referred to as the *RG Model*.
- 1978 - Optoacoustic microscopy and depth profiling of solid samples
- 1982 - Thermoacoustic and optoacoustic imaging of soft (biological) tissues is proposed
- 1990's - Development of the first prototype optoacoustic imagers for breast cancer detection, tissue depth profiling and spectroscopic studies of blood
- 2002 - First *in-vivo* high-resolution optoacoustic tomography imaging studies are demonstrated in mice and rats

The long time it took for the optoacoustic effect to make its way from the accidental discovery by Bell to its eventual place in modern spectroscopy and tomography, is **unique** among the pantheon of physics phenomena.



## The optoacoustic signal



## Thermal expansion

### Conventional ultrasound:

- ▶ Equation of continuity:  $\delta\rho_t + \rho_0\nabla \cdot (\mathbf{u}) = 0$
- ▶ State equation:  $\delta p = c_0^2\delta\rho$

### With thermal expansion

- ▶ Equation of continuity:  $\nabla \cdot (\boldsymbol{\xi}) = -\kappa\delta p + \beta\delta T$   
where  $\boldsymbol{\xi}_t = \mathbf{u}$

## The optoacoustic equation

- ▶ Equation of continuity:  $\nabla \cdot (\boldsymbol{\xi}) = -\kappa\delta p + \beta\delta T$
- ▶ Conservation of momentum:  $\rho_0\boldsymbol{\xi}_{tt} + \nabla\delta p = 0$

The full optoacoustic equation for temperature:

$$\left(\nabla^2 - \frac{1}{c_0^2}\frac{\partial^2}{\partial t^2}\right)p(\mathbf{r}, t) = -\frac{\beta}{\kappa c_0^2}\frac{\partial^2}{\partial t^2}T(\mathbf{r}, t)$$

## Thermal confinement

Heat transfer equation:

$$\nabla^2 T(\mathbf{r}, t) - \frac{\partial}{\alpha \partial t} T(\mathbf{r}, t) = -\frac{1}{k} q(\mathbf{r}, t)$$

Under thermal confinement:

$$\rho C_V \frac{\partial}{\partial t} T(\mathbf{r}, t) = H(\mathbf{r}, t)$$

## The optoacoustic equation under thermal confinement

$$\left( \nabla^2 - \frac{1}{c_0^2} \frac{\partial^2}{\partial t^2} \right) p(\mathbf{r}, t) = -\frac{\beta}{\kappa c_0^2} \frac{\partial^2}{\partial t^2} T(\mathbf{r}, t)$$

$$\rho C_V \frac{\partial}{\partial t} T(\mathbf{r}, t) = H(\mathbf{r}, t)$$

Grüneisen coefficient:

$$\Gamma = \frac{\beta}{\rho C_V \kappa}$$

$$\left( \frac{\partial^2}{\partial t^2} - c_0^2 \nabla^2 \right) p(\mathbf{r}, t) = \frac{\beta}{\rho C_V \kappa} \frac{\partial}{\partial t} H(\mathbf{r}, t)$$

## Frequency-domain solution

$$H(\mathbf{r}, t) = H(\mathbf{r})\delta(t)$$

$$\left( \frac{\partial^2}{\partial t^2} - c_0^2 |\mathbf{k}|^2 \right) p(\mathbf{k}, t) = \Gamma H(\mathbf{k}) \frac{\partial}{\partial t} \delta(t)$$

The solution:  $p(\mathbf{k}, t) = \Gamma H(\mathbf{k}) \cos(c_0 |\mathbf{k}| t)$

For  $t = 0$ :  $p(\mathbf{k}, t = 0) = \Gamma H(\mathbf{k})$   
 $p(\mathbf{r}, t = 0) = \Gamma H(\mathbf{r})$

## Online resources



The screenshot shows the homepage of the k-Wave website at [www.k-wave.org](http://www.k-wave.org). The header features the k-Wave logo with a circular icon of a wave and the text "k-Wave A MATLAB toolbox for the time-domain simulation of acoustic wave fields". Below the header is a navigation menu with links for home, download, installation, license, publications, documentation, and forum. A banner below the menu highlights a "FREE acoustics toolbox for MATLAB". The "Supercomputing 2015" section is visible, along with a "Features" section describing the toolbox's capabilities. To the right, there is a product image of the k-Wave software box.

## 1D solution

$$H(\mathbf{r}, t) = H(z)\delta(t)$$

Frequency domain:

$$p(k_z, t) = \Gamma H(\mathbf{k}) \cos(c_0 k_z t)$$

Time domain:

$$p(z, t) = \Gamma \left[ \frac{H(z - c_0 t)}{2} + \frac{H(z + c_0 t)}{2} \right]$$

## Solution for a slab

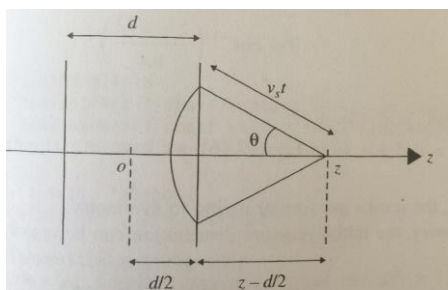


Figure 12.1. Diagram for a slab object.

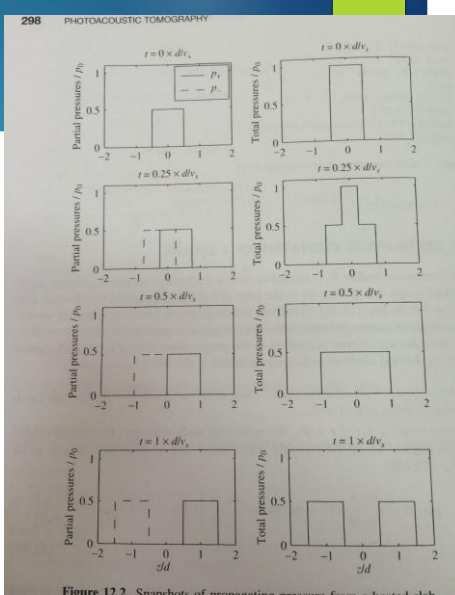


Figure 12.2. Snapshots of propagating pressure from a heated slab.

## 3D solution – Green's function

Source:  $\Gamma \frac{\partial}{\partial t} H(\mathbf{r}, t) = \delta(\mathbf{r})\delta(t)$

Solution:  $p(\mathbf{r}, t) = \frac{\delta(|\mathbf{r}| - c_0 t)}{4\pi|\mathbf{r}|}$

Source:  $H(\mathbf{r}, t) = \delta(\mathbf{r})\delta(t)$

Solution:  $p(\mathbf{r}, t) = \Gamma c_0 \frac{\delta'(|\mathbf{r}| - c_0 t)}{4\pi|\mathbf{r}|}$

## General solution in 3D

General solution:

$$p(\mathbf{r}, t) = \int \frac{\delta(|\mathbf{r} - \mathbf{r}'| - c_0(t - t'))}{4\pi|\mathbf{r} - \mathbf{r}'|} \Gamma \frac{\partial}{\partial t} H(\mathbf{r}', t') d\mathbf{r}' dt'$$

Source:  $H(\mathbf{r}, t) = \delta(\mathbf{r})\delta(t)$

Solution:  $p(\mathbf{r}, t) = \frac{\Gamma}{4\pi c_0} \frac{\partial}{\partial t} \int_{|\mathbf{r}-\mathbf{r}'|=c_0t} \frac{H(\mathbf{r} - \mathbf{r}')}{|\mathbf{r} - \mathbf{r}'|} d\mathbf{r}'$

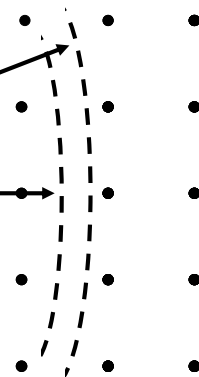
## General solution in 3D

$$p(r, t) = \frac{\Gamma}{4\pi c_0} \frac{\partial}{\partial t} \int_{R=ct} H_r(r') dA',$$

Acoustic  
detector

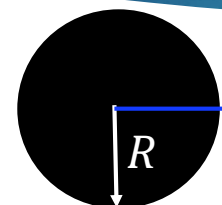
$$R = c(t + \varepsilon)$$

$$R = ct$$

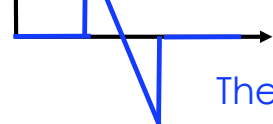


The measured pressure fields  $p(\mathbf{r}, t)$  are projections over spherical shells

## Solution for a sphere



$$p(\mathbf{r}, t) = \begin{cases} 0 & t < \frac{d - R}{c_0} \\ \frac{1}{2d}(d - c_0 t) & \frac{d - R}{c_0} < t < \frac{d + R}{c_0} \\ 0 & \frac{d + R}{c_0} < t \end{cases}$$



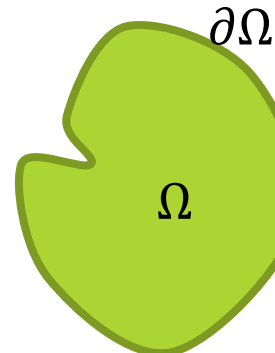
The so-called “N-shaped” signal

## The tomographic problem

Given  $p(\mathbf{r}, t)$  on a closed surface  $\partial\Omega$  find  $p(\mathbf{r}, 0)$  or  $H(\mathbf{r})$  in the enclosed volume  $\Omega$

### Assumptions:

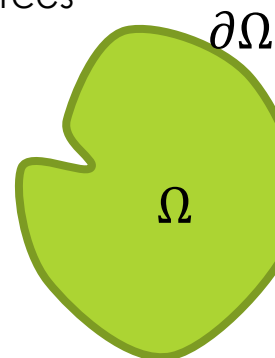
- ▶ Nothing outside the surface
- ▶ Pulse excitation
- ▶ Regularity



## Time-reversal approach

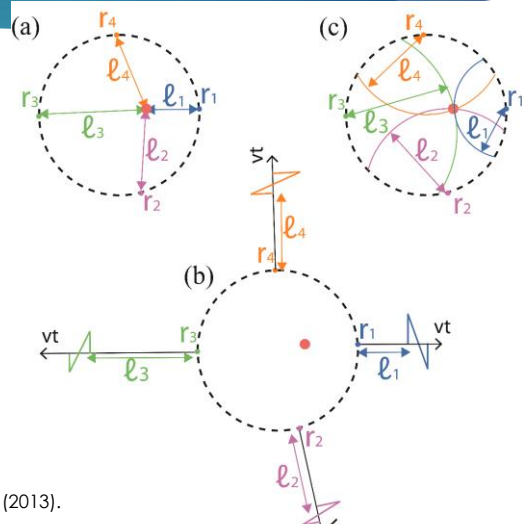
We can reverse the time axis on the wave equation and let the fields propagate from the boundary back to their sources

- Can be used as an inversion algorithms
- Shows that a unique solution exists



## Back-projection algorithms

Back-project each projection on a spherical shell



Rosenthal et al., Curr. Med. Imaging. Rev., 9 (2013).

## Universal back-projection formula

Exact solution for a sphere, cylinder and plane:

$$H(\mathbf{r}) = \frac{2}{\Gamma_S} \int_S \left[ p(\mathbf{r}_s, t) - t \frac{\partial p(\mathbf{r}_s, t)}{\partial t} \right]_{|vt|=|\mathbf{r}_s - \mathbf{r}|} \frac{d\Omega_r(\mathbf{r}_s)}{\Omega_0}$$

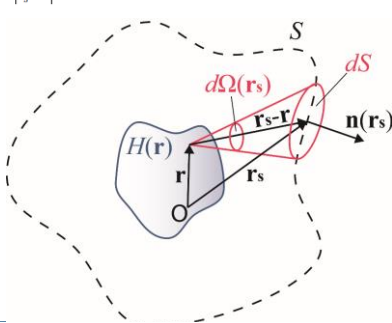
For a sphere:

$$d\Omega_r(\mathbf{r}_s) = dS / |\mathbf{r}_s|^2$$

In the far field:

$$H(\mathbf{r}) \equiv -\frac{1}{2\pi\Gamma_S} \int_S t \frac{\partial p(\mathbf{r}_s, t)}{\partial t} \Big|_{|vt|=|\mathbf{r}_s - \mathbf{r}|} d\Omega_r(\mathbf{r}_s)$$

Rosenthal et al., Curr. Med. Imaging. Rev., 9 (2013).



## Limitations on ultrasound detection

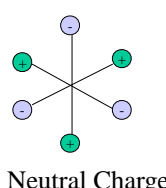
The measurement of  $p(\mathbf{r}, t)$  is not ideal:

- ▶ Finite detector size
- ▶ Sampled data
- ▶ Limited bandwidth
- ▶ Open detection surface
- ▶ Noise

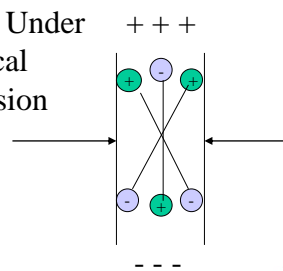
## Piezoelectric effect

In piezoelectric materials, mechanical deformation generates polarization changes

Unit Cell at Rest



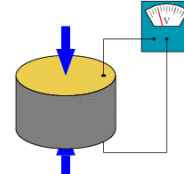
Unit Cell Under Mechanical Compression



## Piezo-electric ultrasound transducers

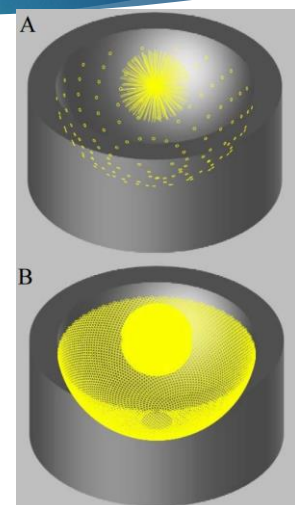
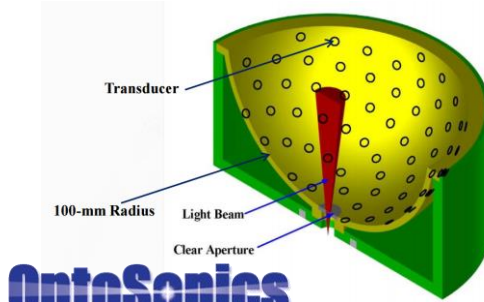
Ultrasound pressure converted to voltage

- ▶ Mature technology
- ▶ Signal proportional to the net deformation within the detector
- ▶ Arrays
- ▶ Acoustic and electric impedances matter



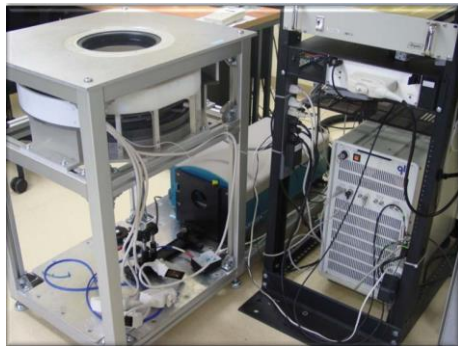
## Spherical detection systems

- ▶ Half a sphere
- ▶ Rotation increases proj. # (but takes time)

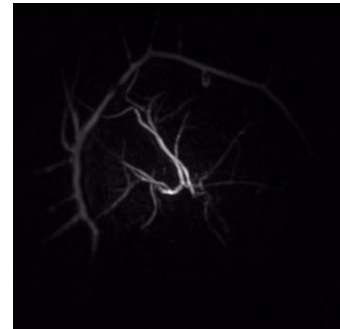


## Breast imaging

System

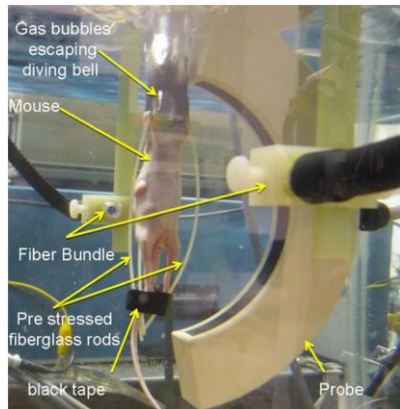


Breast vasculature

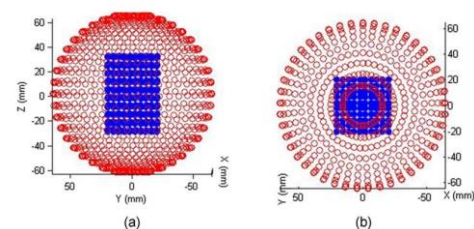


**OptoSonics**

## Small animal imager

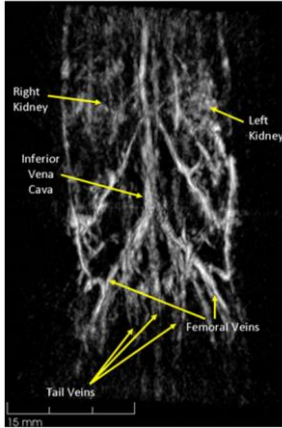


Scanning gives a whole tomographic view

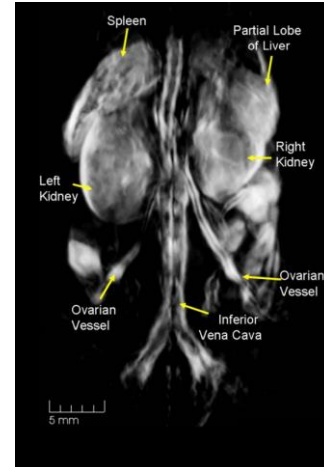


H. P. Brecht *et al.* JBO 14 (2009)

## Reconstructions

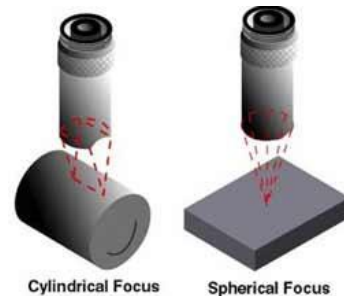


H. P. Brecht et al. JBO 14 (2009)



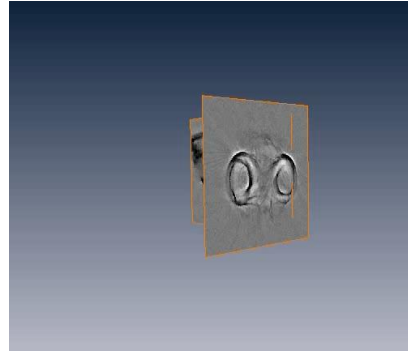
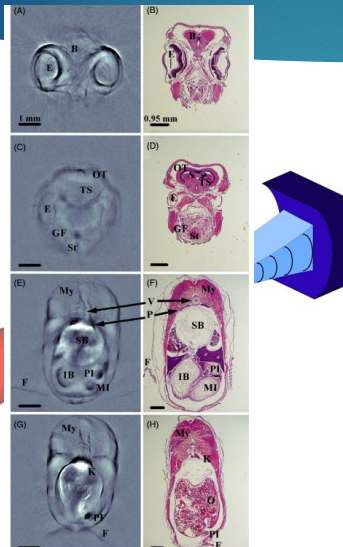
## Cylindrical focusing

- ▶ In 3D systems, many projections are needed -> slow imaging
- ▶ Using cylindrical focusing (focusing to a plane), a 2D tomographic problem is obtained



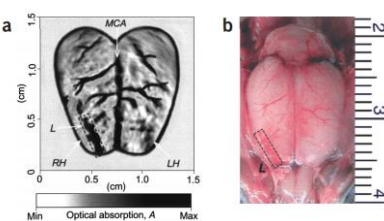
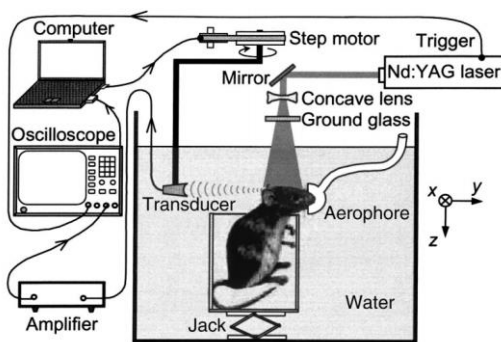
<https://www.nde-ed.org/EducationResources/CommunityCollege/Ultrasonics/EquipmentTrans/transducertypes.htm>

## Example: Imaging of Zebrafish



R. Ma et al. Phys. Med. Biol. 57 (2012)

## Example: Imaging of mouse brain



X. Wang et al. Nature Biotech. 21 (2003).

## Real time 2D imaging - preclinical



Razansky et al., *Nature Protoc.*, **6**, 2011  
<http://www.ithera-medical.com/>

## Real time 2D imaging

Number of required projections is low enough to enable parallel detection



Buehler et al., *Optics Letters*, **38**(9), 2013.



## Central slice theorem

Projection equation:

$$g(r, \theta) = \iint_D f(x, y) \delta(r - x \cos \theta - y \sin \theta) dx dy$$

Fourier transforms:

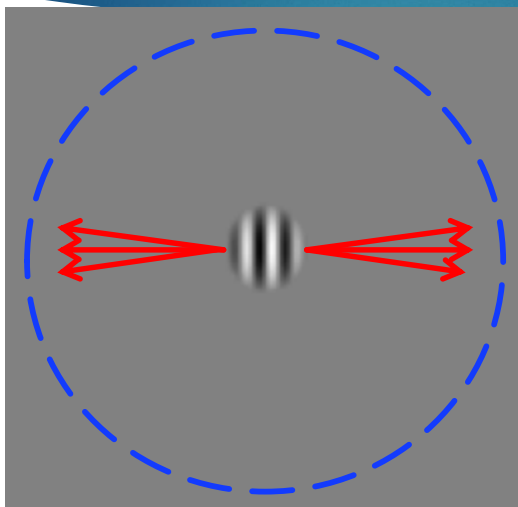
$$\hat{g}_\theta(k) = \int_{-\infty}^{\infty} g(r, \theta) e^{-2\pi k r} dr$$

$$\hat{f}(k_x, k_y) = \int_{-\infty}^{\infty} f(x, y) e^{-2\pi (k_x x + k_y y)} dx dy$$

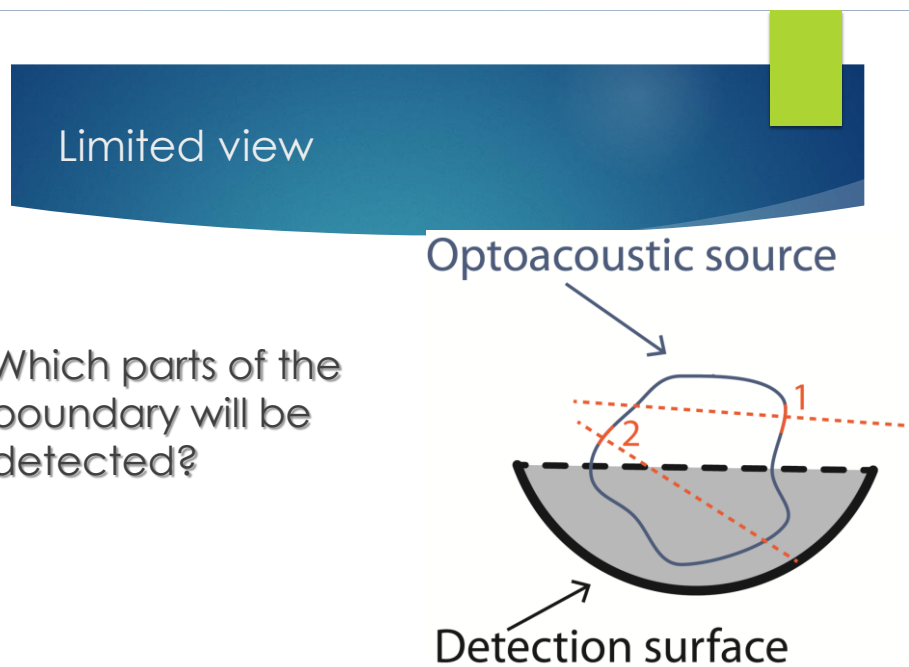
Central slice theorem:

$$\hat{g}_\theta(k) = \hat{f}(k \cos \theta, k \sin \theta)$$

## Image directivity in optoacoustics



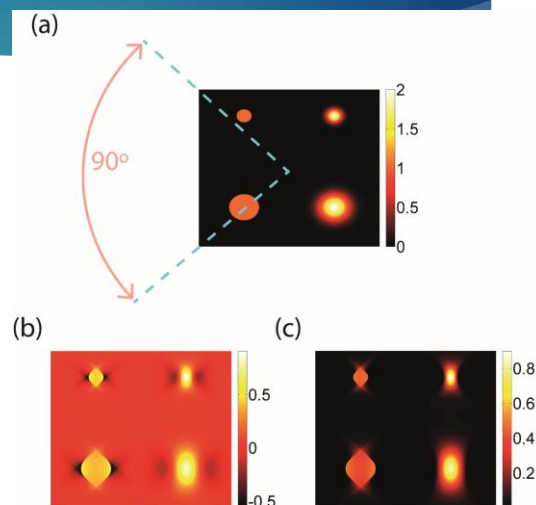
**Directivity is a result of spatial frequencies in the object**



Rosenthal et al., Curr. Med. Imaging. Rev., 9 (2013).

### Limited view - example

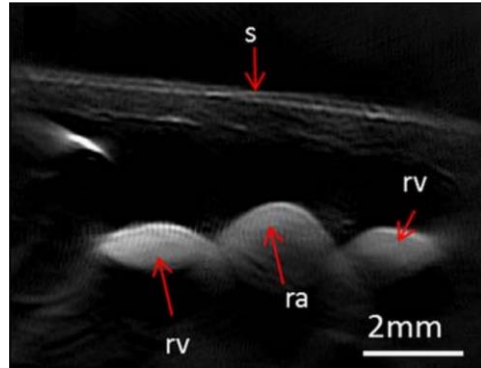
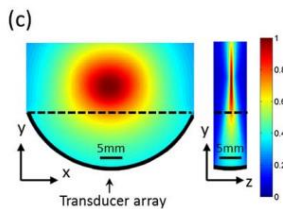
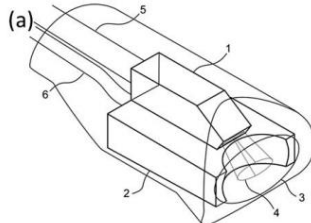
Originating image:



Reconstructions:

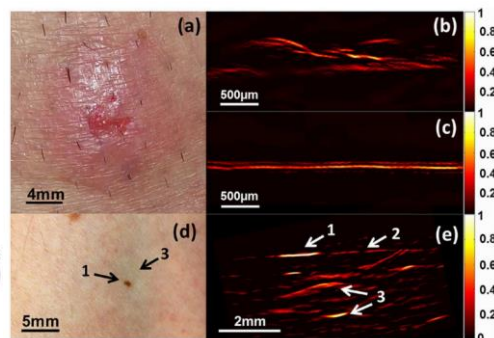
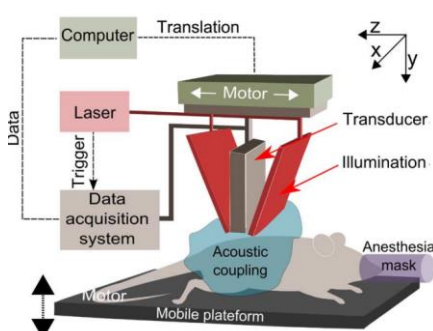
Rosenthal et al., Curr. Med. Imaging. Rev., 9 (2013).

## The effect of limited view in cross-sectional systems



Buehler et al., Optics Letters, 38(9), 2013.

## The effect of limited view in cross-sectional systems



L. Vionnet et al. IEEE TMI 33 (2013)

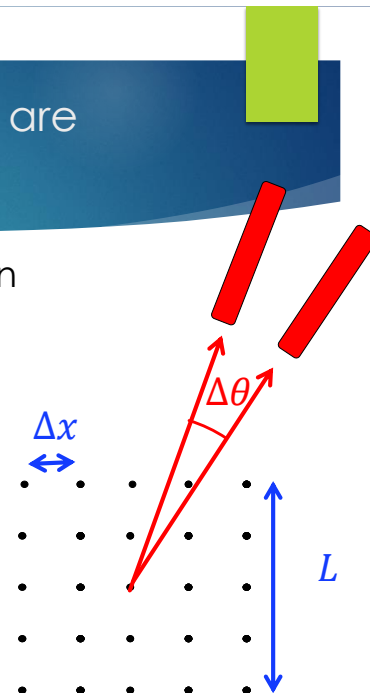
How many projections are needed?

Using the far-field approximation and the central-slices theorem:

$$\Delta\theta = \frac{\Delta x}{L}$$

$$N_\theta = \pi N_x$$

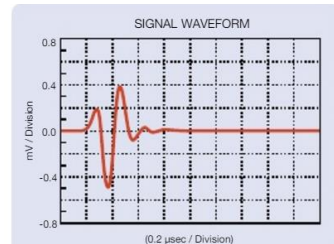
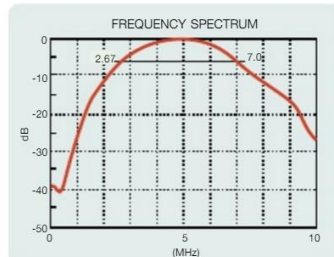
An image of 100x100 would ideally require 314 projections (practically fewer)



Electro-mechanical impulse/frequency response

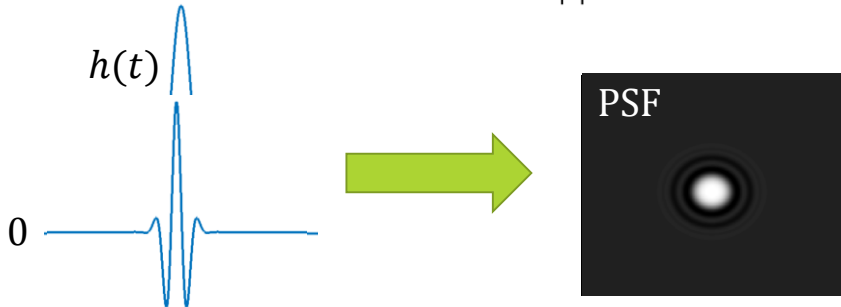
$$p_{\text{det}}(t) = h(t) * p(t)$$

- ▶ The impulse response  $h(t)$  depends on the mechanical and acoustic impedances of the piezoelectric transducer
- ▶ Transducers often have an acoustic resonance



## Electro-mechanical impulse/frequency response

The image is convolved with the isotropic point spread function (PSF):  $\text{PSF} = -\frac{1}{4\pi|\mathbf{r}|} [h'(|\mathbf{r}|/c_0) + h'(-|\mathbf{r}|/c_0)]$

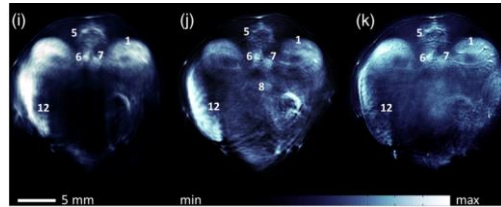


## Transducer bandwidth and data sampling rate

- ▶ To image at a resolution  $\Delta r$ , the temporal sampling step should be  $\sim \Delta r/c_0$  and the transducer bandwidth should be  $\sim \frac{c_0}{2\Delta r}$ .
- ▶ Example: to image at 15  $\mu\text{m}$ , we need: 50 MHz transducer and 100 MS/s sampling rate.

## Negative image values

- ▶ The optoacoustic image represents energy absorption -> positive values expected
- ▶ Negative values obtained because:
  - ▶ Transducer (negative) impulse response
  - ▶ Limited view
  - ▶ Artifacts



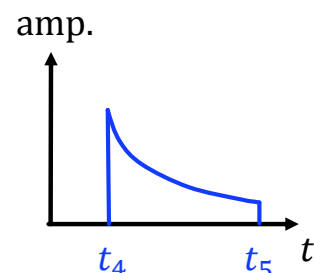
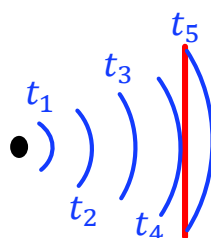
A. Dima et al. JBO 19 (2014)

## Geometrical effects of finite detector sizes

### Simple model: spatial averaging

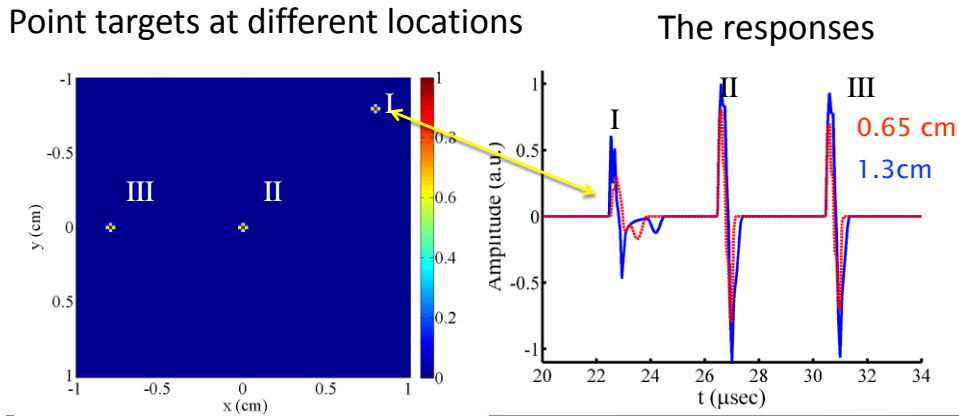
$$p_{detect}(t) = \int p(r, t) D(r) dr,$$

$$D(r) = \begin{cases} 1 & r \in \text{detector area} \\ 0 & \text{else} \end{cases}$$



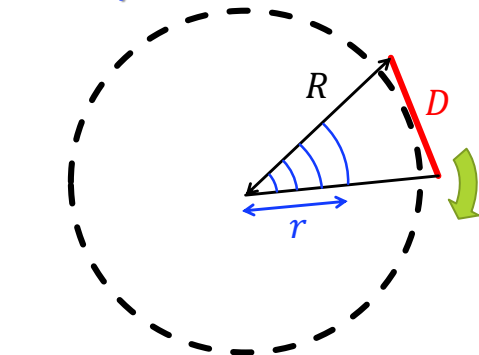
## Finite detector: effect on signal

The response is spatially dependent

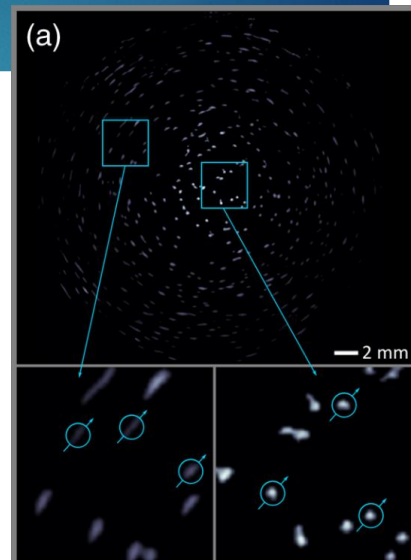


## Finite detector: effect on reconstruction

Tangential smearing  
of  $Dr/R$

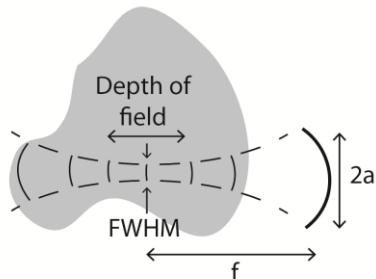


A. Dima et al. JBO 19 (2014)



## The limits of acoustic focusing

**Diffraction always limits resolution**

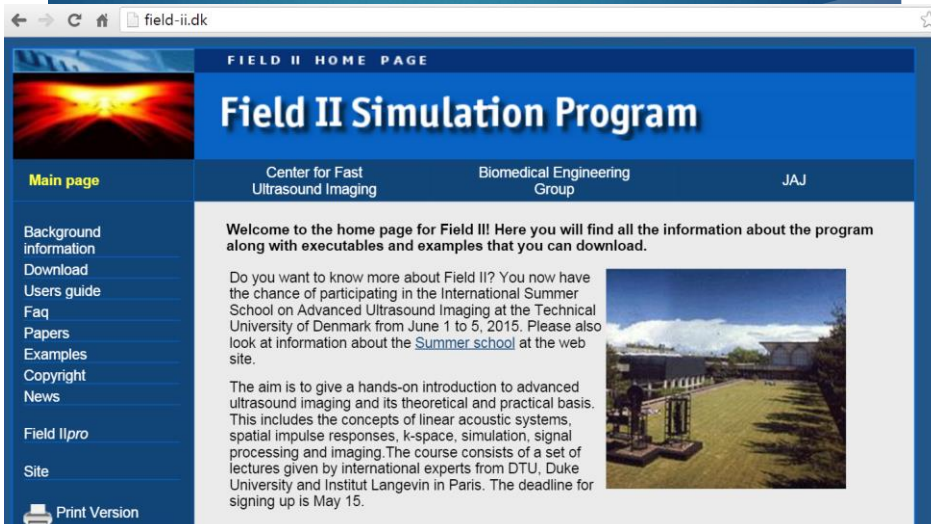


$$\text{FWHM} = 1.41\lambda \cdot f / 2a$$

$$\text{DOF} = 9.7\lambda \cdot (f / 2a)^2$$

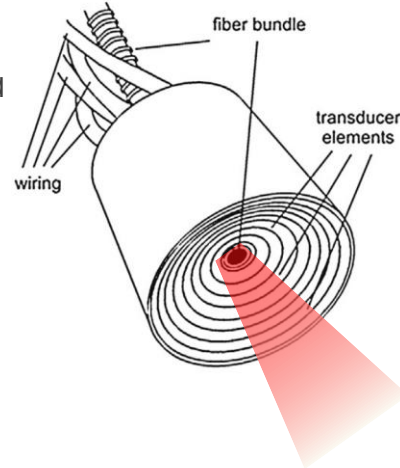
$\lambda$  is the acoustic wavelength or optoacoustic feature size

## Finite detector size: online resources



## 3D real time

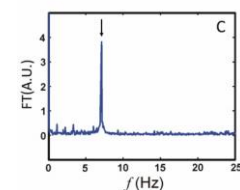
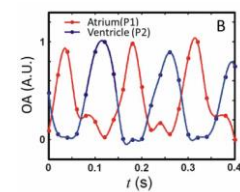
- ▶ 256-512 projections
- ▶ Good resolution only in a small field of view



Deán-Ben & Razansky, Photoacoustics, 1, 2013.

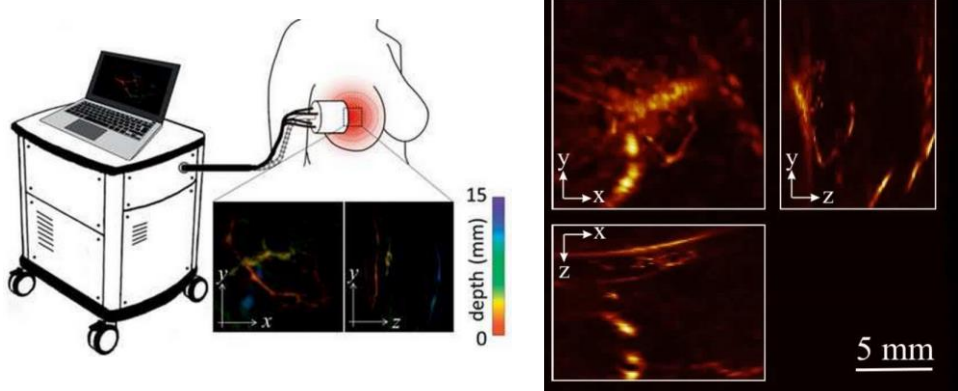
## Application: Cardiac imaging in mice

### Heart-rate analysis

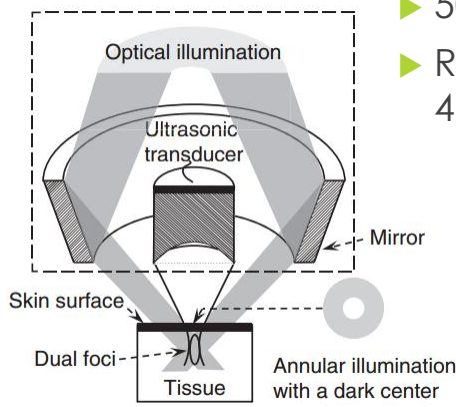


Deán-Ben et al. Scientific Reports, 5, 2015

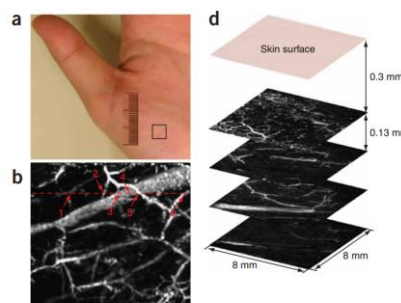
## Imaging of breast vasculature



## Focused transducers for optoacoustic microscopy (acoustic resolution)



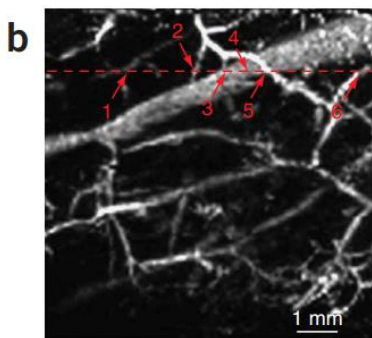
- ▶ 50 MHz transducer
- ▶ Resolution: 15  $\mu\text{m}$  axial, 45  $\mu\text{m}$  lateral



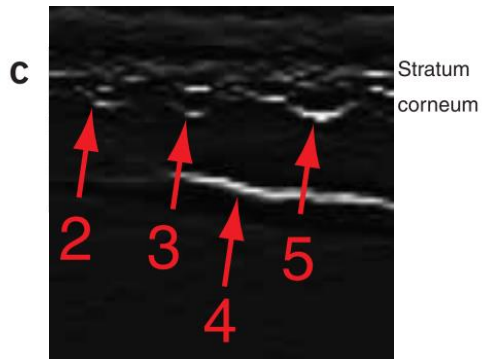
H. F. Zhang et al. Nature Biotechnology 24 (2006)

## Resolution in optoacoustic microscopy

Lateral image (MAP)

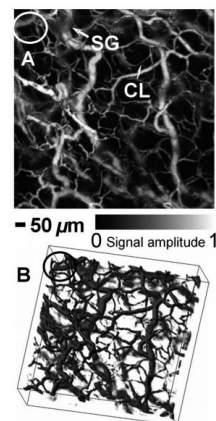
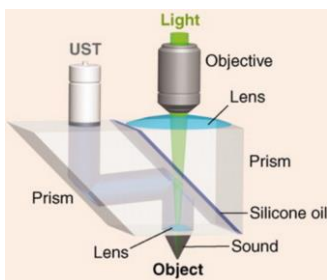


Axial image



H. F. Zhang et al. Nature Biotechnology 24 (2006)

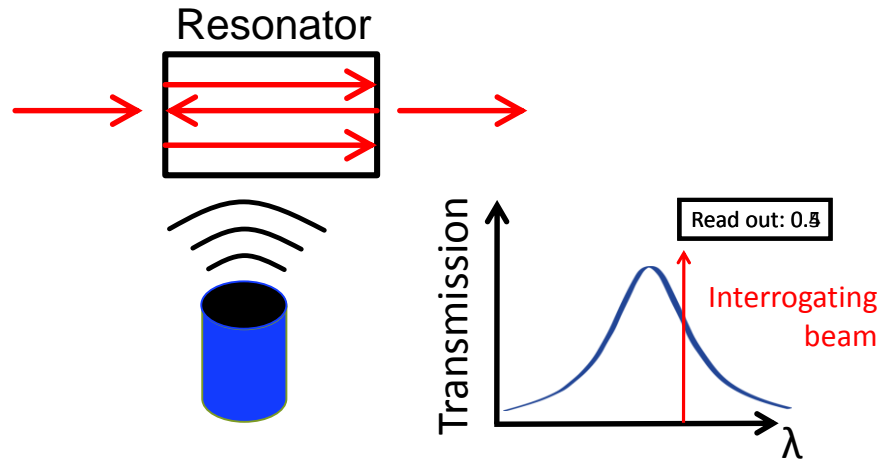
## Optical focusing in optoacoustic imaging (optical resolution)



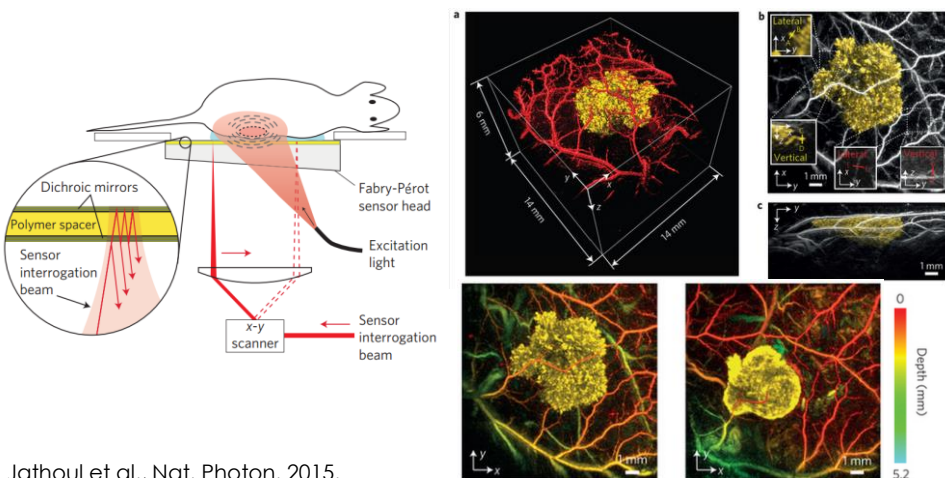
- ▶ Sub-micron resolution (single blood cells imaged in high res.)
- ▶ Limited by optical scattering

K. Maslov et al. Opt. Lett. 33 (2008)  
L. V. Wang and S. Hu, Science 335 (2012)

## Optical detection of ultrasound



## Optoacoustic tomography using a planar Fabry-Pérot



Jathoul et al., Nat. Photon. 2015.

## Acoustic attenuation

$$\alpha(f) = \alpha_0 |f|^n$$

### Typical values

Material	Propagation speed, $c$ (m s $^{-1}$ )	Characteristic impedance, $Z$ (10 $^6$ kg m $^{-2}$ s $^{-1}$ )	Attenuation coefficient, $\alpha$ at 1 MHz (dB cm $^{-1}$ )	Frequency dependence of $\alpha$	Nonlinear parameter, $B/A$
Air	330	0.0004	1.2	$f^2$	
Blood	1570	1.61	0.2	$f^{1.3}$	6.1
Brain	1540	1.58	0.9	$f$	6.6
Fat	1450	1.38	0.6	$f$	10
Liver	1550	1.65	0.9	$f$	6.8
Muscle	1590	1.70	1.5–3.5	$f$	7.4
Skull bone	4000	7.80	13	$f^2$	
Soft tissue (mean values)	1540	1.63	0.6	$f$	
Water	1480	1.48	0.002	$f^2$	5.2

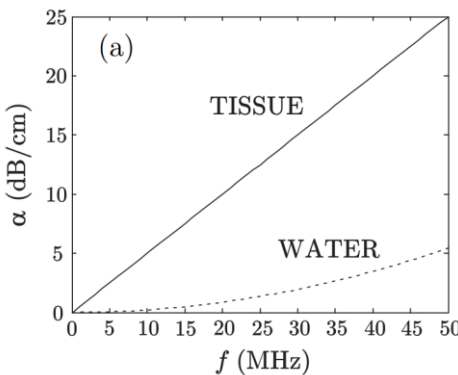
In water: due to viscosity

P. N.T. Wells Rep. Prog. Phys. **62** (1999)

In tissue: due to scattering

## Typical acoustic attenuation in tissue

$$\alpha = 0.6 \text{ dB cm}^{-1} \text{MHz}^{-1}$$



### Conclusion:

Penetration depth is inversely proportional to frequency (resolution)

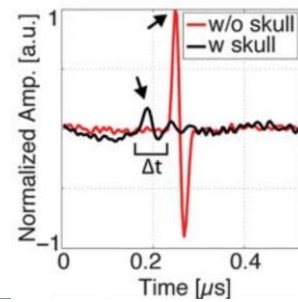
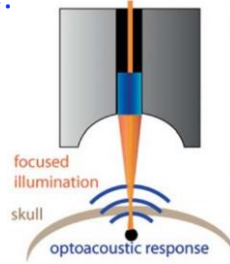
X. L. Dean-Ben et al., Phys. Med. Bio. **56** (2011)

## Acoustically absorbing organs

- ▶ Respiratory system (lungs especially)
- ▶ Bones (skull especially)

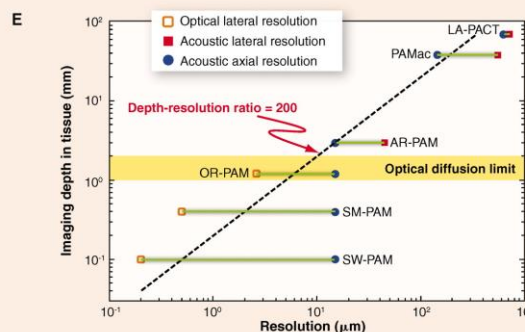
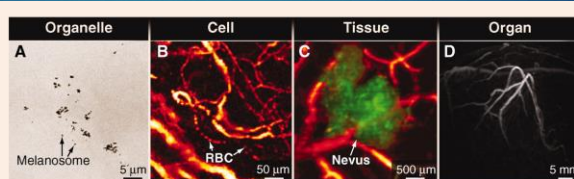
Mouse skull example:

M. Kneip et al. J. Biophotonics (2015)



## Depth-resolution ratio

L. V. Wang and S. Hu,  
Science 335 (2012)



## Model-based approach to optoacoustic image reconstruction

- ▶ Analytical tomographic inversion formulae assume ideal detection conditions
- ▶ Proper modeling can in the following cases:
  - ▶ Finite detector size
  - ▶ Acoustic attenuation/heterogeneities
  - ▶ Limited detection angle

## Model-based approach to optoacoustic image reconstruction

Continuous model:

$$p(r, t) = \frac{\Gamma}{4\pi c_0} \frac{\partial}{\partial t} \int_{R=ct} \frac{H_r(r')}{R} dA' + p_{\text{det}}(\mathbf{r}, t) = h(t) * \int_S P(\mathbf{r}, t) D(\mathbf{r}) dS$$

Discrete model:  $\mathbf{p} = \mathbf{M}\mathbf{h}$

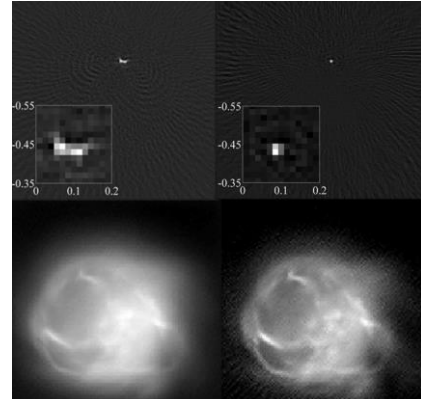
$$\mathbf{h}_{\text{sol}} = \arg \min_u \|\mathbf{p} - \mathbf{M}\mathbf{h}\|_2^2$$

## Model-based image enhancement

For finite aperture detectors, proper modeling can enhance lateral resolution

Hair

Partial model      Full model



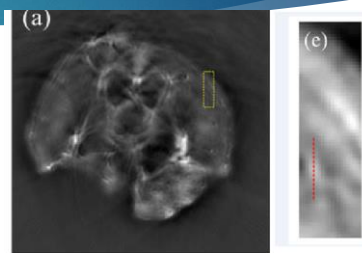
Mouse

A. Rosenthal *et al.* Med. Phys. **38** (2011)

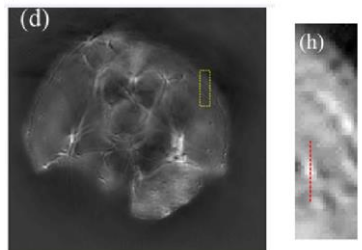
## Model-based image enhancement

Regularization can reduce artifacts and enhance features

Standard



Regularized



Y. Han *et al.* Med. Phys. **42** (2015)

What is the optoacoustic image?

$$\left( \frac{\partial^2}{\partial t^2} - c_0^2 \nabla^2 \right) p(\mathbf{r}, t) = \Gamma H(\mathbf{r}) \frac{\partial}{\partial t} \delta(t)$$

$H(\mathbf{r})$  is the total energy density deposited the tissue

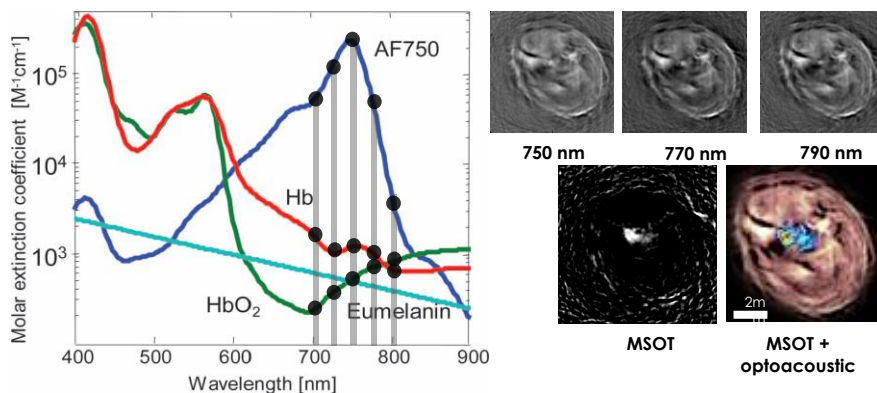


$$H(\mathbf{r}) = \eta_{\text{th}} \mu_a(\mathbf{r}, t) u(\mathbf{r})$$

$u(\mathbf{r})$  is the fluence

$\eta_{\text{th}}$ : thermal efficiency

Multi-spectral optoacoustic tomography (MSOT)



## Spectral unmixing

$$\mu_a(\lambda_n) = \sum_{m=1}^M a_m(\lambda_n)c_m, \quad n = 1, \dots, N$$

$$\begin{pmatrix} \mu_a(\lambda_1) \\ \vdots \\ \mu_a(\lambda_n) \end{pmatrix} = \begin{bmatrix} a_1(\lambda_1) & \cdots & a_m(\lambda_1) \\ \vdots & \ddots & \vdots \\ a_1(\lambda_n) & \cdots & a_m(\lambda_n) \end{bmatrix} \begin{pmatrix} c_1 \\ \vdots \\ c_m \end{pmatrix}$$

$\mu = \mathbf{Ac}$

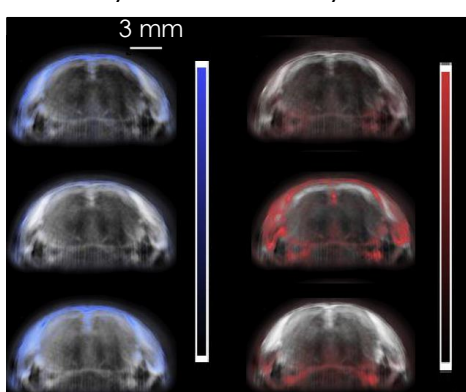
known spectra      unknown spectra

$$\mathbf{c}_{\text{sol}} = \text{argmin} \|\mu - \mathbf{Ac}\| \quad \text{blind unmixing: PCA, ICA}$$

J. Glatz et al. Opt. Express 19 (2011)

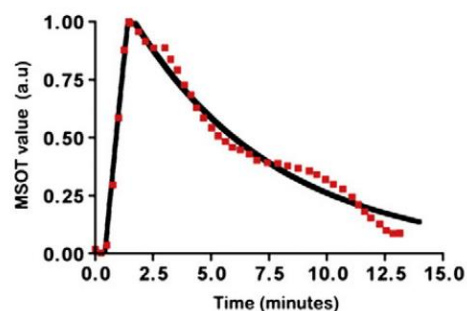
## Functional brain imaging

Deoxy-Hb



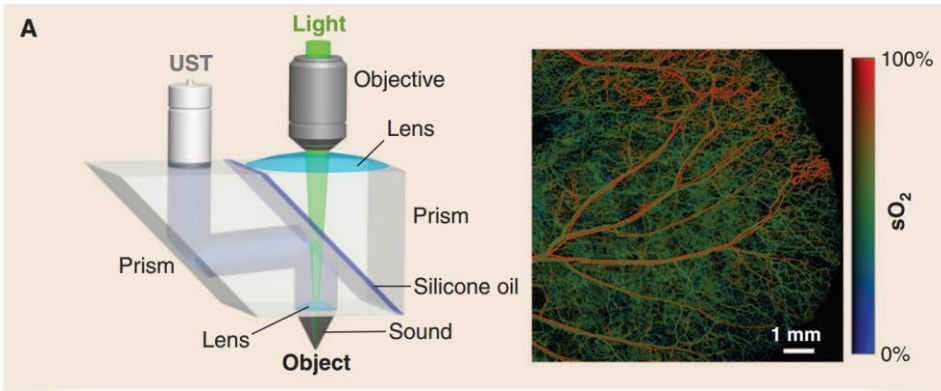
Oxy-Hb

ICG injection



N. C. Burton, et al. Neuroimage, 35, 2013.

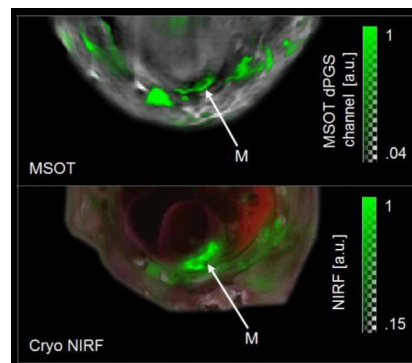
## Functional optoacoustic microscopy



L. V. Wang and S. Hu, Science 335 (2012)

## Molecular imaging: injectable dyes

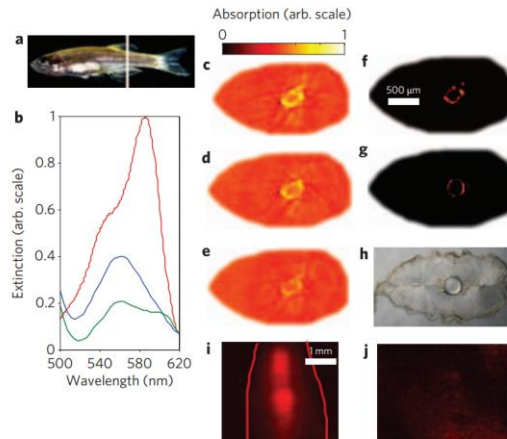
Myocardial infarction resolved with dPGS fluorescent agent targeted to P- and L-selectin



Taruttis et al., Photoacoustics 1, 2013.

## Molecular imaging: fluorescent proteins

mCherry distribution in the vertebral column of an **adult** zebrafish



D. Razansky et al., Nat. Photon. **3**, 2009

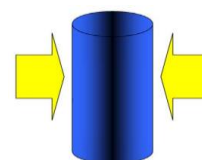
## The fluence

$$H(\mathbf{r}) = \eta_{\text{th}} \mu_a(\mathbf{r}) u(\mathbf{r})$$

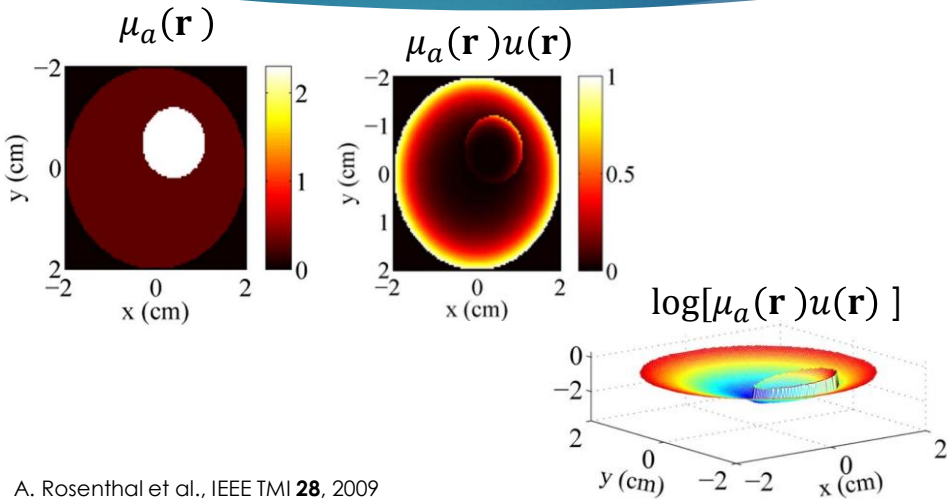
fluence rate:  $U(\mathbf{r}, t) = \int_{4\pi} I(\mathbf{r}, \hat{\mathbf{s}}, t) d\Omega$  (W/cm<sup>2</sup>)

fluence:  $u(\mathbf{r}) = \int U(\mathbf{r}, t) dt$  (J/cm<sup>2</sup>)

In thick tissue, the fluence decays exponentially

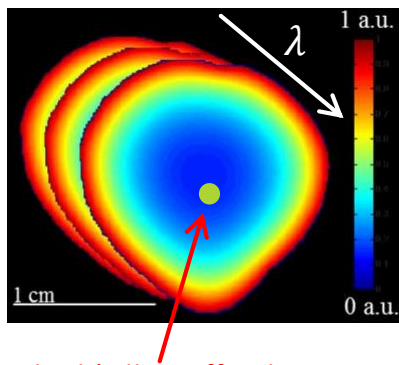


## The spatial effect the fluence: example

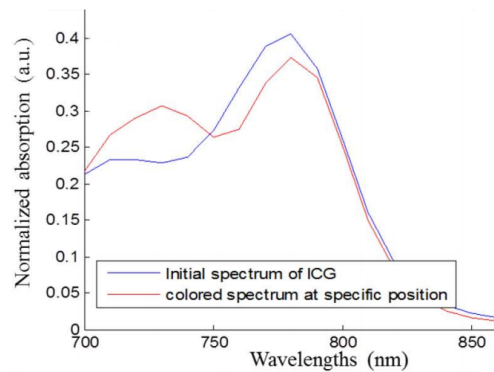


## The spectral effect of fluence

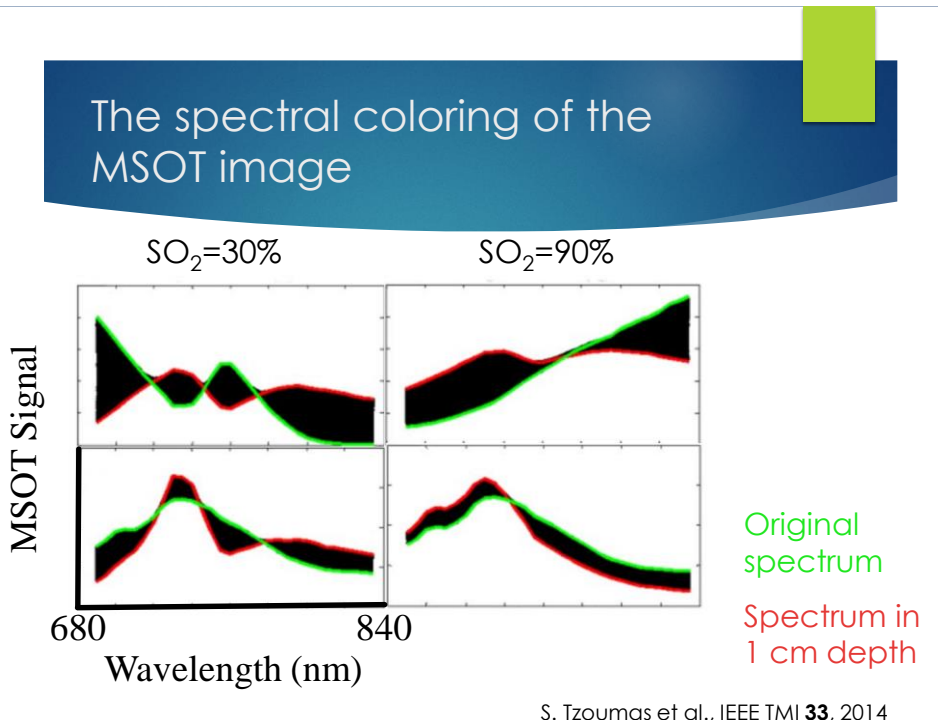
The fluence depends on  $\lambda$



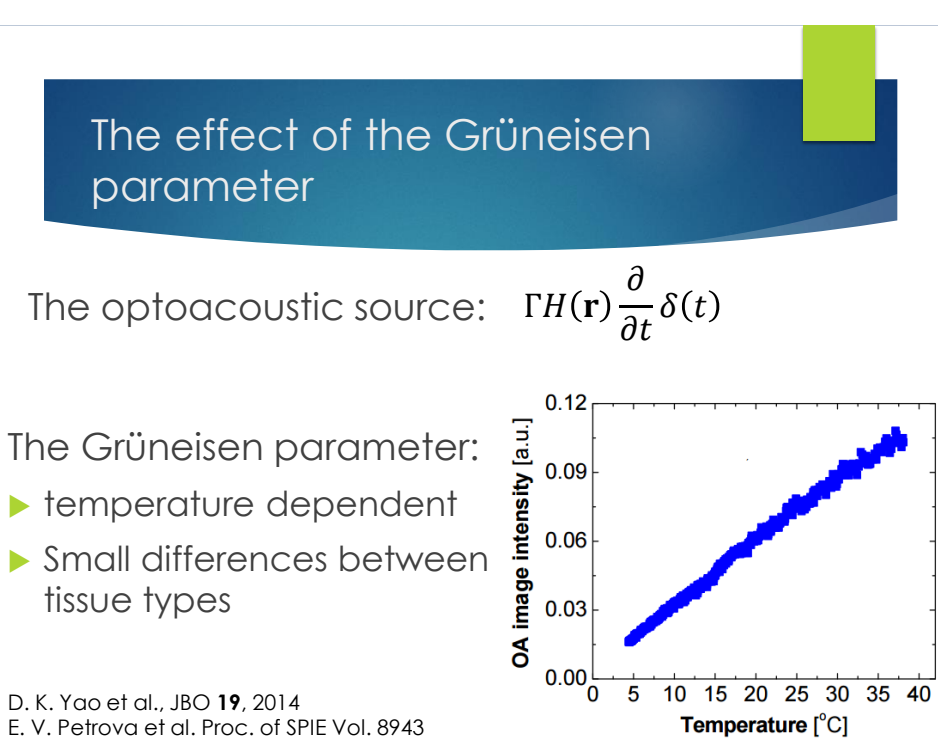
What is the effect on a  
deep seated target?



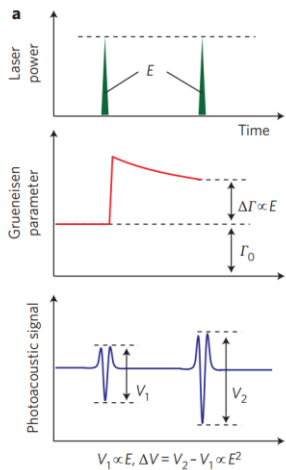
S. Tzoumas et al., IEEE TMI **33**, 2014



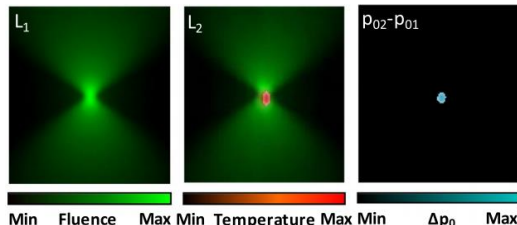
S. Tzoumas et al., IEEE TMI **33**, 2014



## Grueneisen Relaxation Photoacoustic Microscopy (optical resolution)

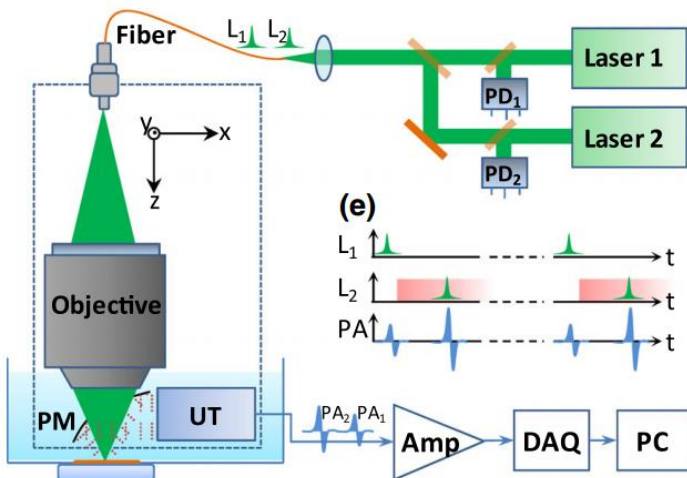


- ▶ The first pulse increases the Grueneisen coefficient
- ▶ A second pulse generates a stronger signal



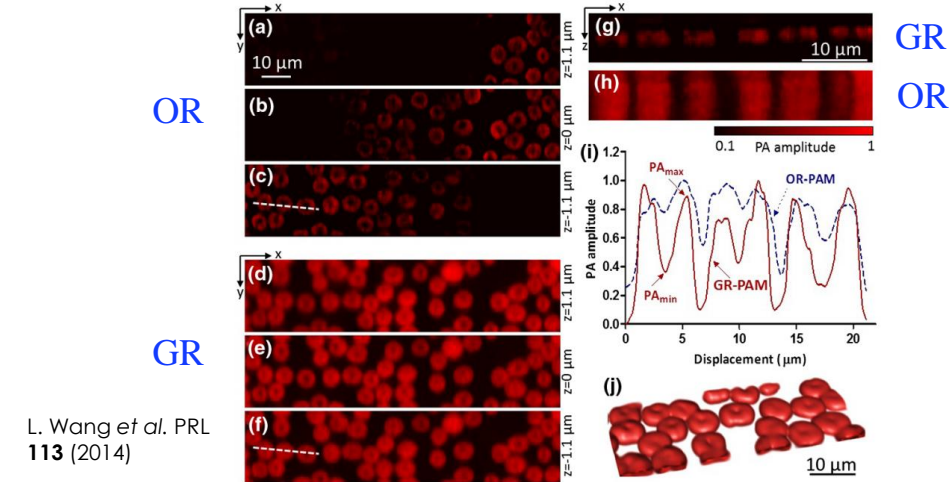
P. Lai et al. Nature Photonics 9 (2015)  
L. Wang et al. PRL 113 (2014)

## Grueneisen Relaxation Photoacoustic Microscopy

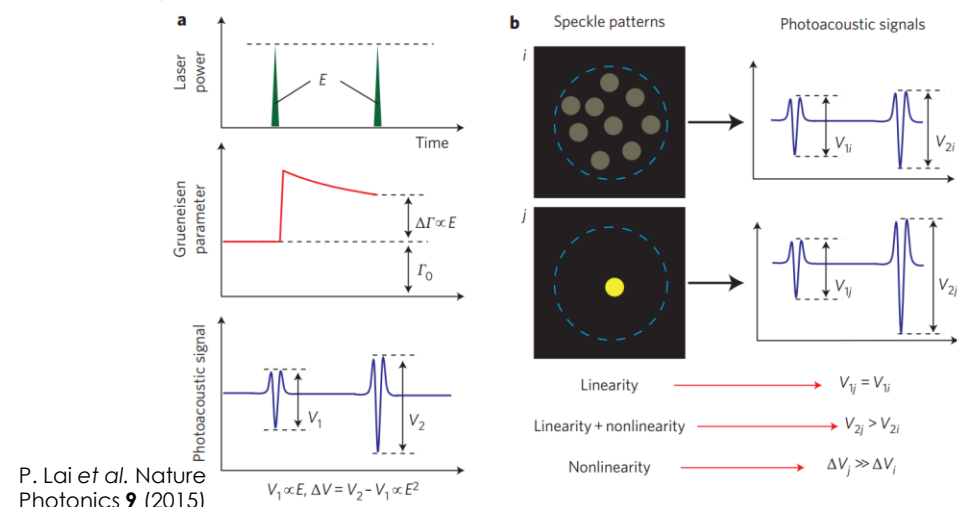


L. Wang et al. PRL 113 (2014)

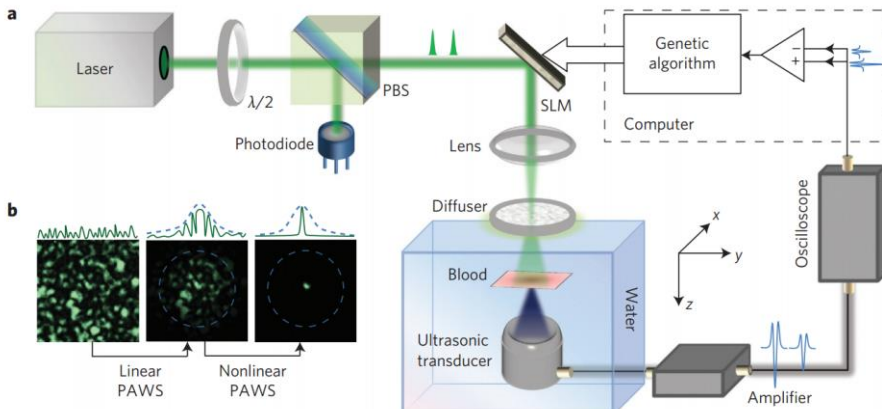
## Grueneisen Relaxation Photoacoustic Microscopy



## Wavefront shaping with Grueneisen relaxation



## Wavefront shaping with Grueneisen relaxation

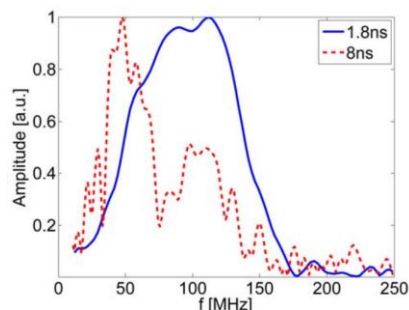


P. Lai et al. Nature Photonics 9 (2015)

## The temporal illumination profile

- ▶ For broad pulses:  $\Gamma H(\mathbf{r}) \frac{\partial}{\partial t} H(t)$
- ▶ The measured signal:  $p(t) = p_\delta(t) * H(t)$

- ▶ Shorter pulses can excite higher frequencies and yield higher res.



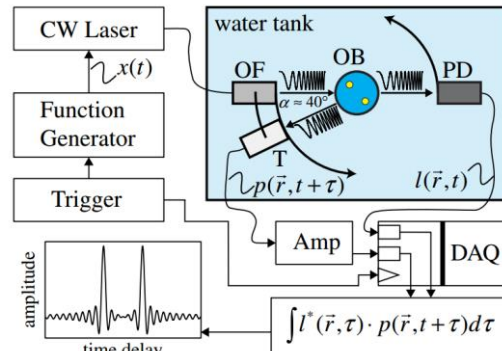
M. Omar et al., Opt. Lett. 38, 2013

## Frequency-domain optoacoustic imaging

$H(t)$  should contain all the frequencies of interest – must not be a  $\delta$ -like pulse

Example: excitation with chirped pulses

S. Kellnberger et al. Opt. Lett. **37** (2012)



## Frequency-domain optoacoustic imaging: SNR

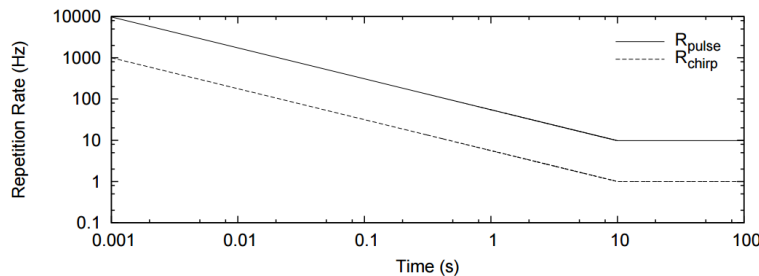


Fig. 4. The optimum repetition rates for a short pulse and a 1 ms chirp pulse.

### 7. Conclusion

We have shown that the SNR of photoacoustic imaging systems based on CW lasers with a chirped modulation frequency are about 20 dB to 30 dB worse than systems based on pulsed lasers if we are constrained by the ANSI safety limits.

A. Petschke et al. Biomed Opt. Express. **1** (2010)